IMPROVING HAND AND WRIST ACTIVITY DETECTION USING TACTILE SENSORS AND TENSOR REGRESSION METHODS ON RIEMANNIAN MANIFOLDS

Noémie Jaquier[1], Claudio Castellini[2] and Sylvain Calinon[1]

[1]*Idiap Research Institute, Martigny, Switzerland*
[2]*DLR - German Aerospace Center, Wessling, Germany*

ABSTRACT

Simultaneous and proportional control of a prosthetic hand and wrist is still a challenging issue, although giant steps have lately been made in this direction. In this paper, we study the application of a novel machine learning method to the problem, with the aim to potentially improve such control. Namely we apply different kernels for tensor Gaussian process regression to data obtained from an advanced, flexible tactile sensor applied on the skin, recording muscle bulging in the forearm. The sensor is a modular, compact bracelet comprising 320 highly sensitive elements organized as a tactile array. The usage of kernel functions with tensor arguments and kernel distances computed on Riemannian manifolds enables us to account for the underlying structure and geometry of the tactile data. Regression accuracy results obtained on data previously collected using the bracelet demonstrate the effectiveness of the approach, especially when using Euclidean distance and Kullback-Leibler divergence-based kernels.

INTRODUCTION

Despite recent advances in externally-powered prosthetics, intuitive and robust control of polyarticulated prosthetic hands and wrists by amputees remains an unsolved problem, mainly due to unadapted user interfaces and inadequate sensorization [1]. Despite remarkable advanced in this direction, e.g., [2, 3, 4], a full, clinically accepted application still has to appear. The recent results of the ARM competition of the Cybathlon, won by Robert Radocy of TRS Prosthetics wearing a body-powered prosthesis[1], stand as a powerful warning for the scientific community.

In this paper, we advance the usage of *tactile sensing* or tactile myography (TMG) to detect hand and wrist movement in a non-invasive way in order to replace or augment the traditional surface electromyography (sEMG). We bring the qualitative analysis of TMG data performed in [5] one step further, by studying regression methods allowing to account for the structure and the geometry of the muscle bulging data. This is enforced using *tensor Gaussian Process Regression*, a technique consisting of predicting a posterior Gaussian density for new inputs knowing a set of input and output data.

We first describe the proposed regression method, then we quickly review the experimental setup and data collection process, and lastly we present our experimental results. A quick discussion completes the paper.

PROPOSED APPROACH

Mathematical background

Gaussian Processes (GP) are a class of probabilistic models that defines a posterior over functions given a set of input and output data. The distribution is assumed to be Gaussian with some mean and covariance. The covariance is computed using a kernel function as a measure of similarity. The idea behind GP is that if two input points are similar according to the kernel, the output of the function at those points will also be similar [6].

Tensors are generalization of vectors and matrices to higher dimensions. They provide an efficient and natural way to represent structured multidimensional data such as videos sequences or electroencephalography (EEG) data. Recently, regression methods have been extended to tensor data, allowing an efficient exploitation of their structure, see for example [7, 8].

Riemannian manifolds are mathematical spaces that locally resemble a Euclidean space. A Riemannian manifold is a smooth manifold whose tangent space is equipped with an inner product [9]. Such model conserves the underlying geometry of the data. Examples of well known manifolds are the surface of hyperspheres (to represent orientations), the space of symmetric positive definite (SPD) matrices [10], or the space of p-dimensional subspaces in a n-dimensional Euclidean space called the Grassmann manifold [11].

Tensor Gaussian Process Regression

Given a dataset of N observations $\{(\boldsymbol{\mathcal{X}}_n, \boldsymbol{y}_n)\}_{n=1}^N$, concatenated as $\boldsymbol{\mathcal{X}} \in \mathbb{R}^{N \times I_1 \times \ldots \times I_m}$ and $\boldsymbol{Y} \in \mathbb{R}^{N \times J}$, we are interested in making prediction for a new input $\boldsymbol{\mathcal{X}}_*$. By extending GP regression to tensor inputs, the predictive dis-

[1]see `http://www.cybathlon.ethz.ch/de/cybathlon-news/resultate/arm-resultate.html` as well as `http://www.trsprosthetics.com`.

tribution of $\boldsymbol{y}_*$ corresponding to $\boldsymbol{\mathcal{X}}_*$ can be inferred as

$$\boldsymbol{y}_*|\boldsymbol{\mathcal{X}}_*, \boldsymbol{\mathcal{X}}, \boldsymbol{Y}, \boldsymbol{\theta} \quad \sim \quad \mathcal{N}(\overline{\boldsymbol{y}}_*, \mathrm{cov}(\boldsymbol{y}_*)), \tag{1}$$

where

$$\begin{aligned} \overline{\boldsymbol{y}}_* &= k(\boldsymbol{\mathcal{X}}_*, \boldsymbol{\mathcal{X}})\big(k(\boldsymbol{\mathcal{X}}, \boldsymbol{\mathcal{X}}) + \sigma^2 \boldsymbol{I}\big)^{-1} \boldsymbol{Y}, \\ \mathrm{cov}(\boldsymbol{y}_*) &= k(\boldsymbol{\mathcal{X}}_*, \boldsymbol{\mathcal{X}}_*) \\ &\quad - k(\boldsymbol{\mathcal{X}}_*, \boldsymbol{\mathcal{X}})\big(k(\boldsymbol{\mathcal{X}}, \boldsymbol{\mathcal{X}}) + \sigma^2 \boldsymbol{I}\big)^{-1} k(\boldsymbol{\mathcal{X}}, \boldsymbol{\mathcal{X}}_*), \end{aligned} \tag{2}$$

and $(\boldsymbol{K})_{ij} = k(\boldsymbol{\mathcal{X}}_i, \boldsymbol{\mathcal{X}}_j)$ is the covariance or kernel matrix [12, 13].

Kernels with tensor inputs on manifolds: In order to exploit both the structure and the geometry of tensor inputs, the kernel is defined as a product of M positive semi-definite factor kernels

$$k(\boldsymbol{\mathcal{X}}, \boldsymbol{\mathcal{X}}') = \prod_{m=1}^{M} k(\boldsymbol{X}_{(m)}, \boldsymbol{X}'_{(m)}), \tag{3}$$

where $\boldsymbol{X}_{(m)} \in \mathbb{R}^{I_m \times I_1 I_2 \ldots I_M}$ is the mode-m matricization or unfolding of tensor $\boldsymbol{\mathcal{X}}$ [12, 13]. Each factor kernel measures the similarity between mode-m unfolding of two tensors. We consider factor kernels in the form of Radial Basis Function (RBF) kernels defined as

$$k(\boldsymbol{X}_{(m)}, \boldsymbol{X}'_{(m)}) = \exp\left(-\frac{d(\boldsymbol{X}_{(m)}, \boldsymbol{X}'_{(m)})}{2\beta_m^2}\right), \tag{4}$$

where $d(\boldsymbol{X}_{(m)}, \boldsymbol{X}'_{(m)})$ is a distance measure. Kernels based on different distances for matrices are presented below.

Kernels based on Kullback-Leibler divergence: The Kullback-Leibler divergence measures the difference between two probability distributions p and q. In our case, each $\boldsymbol{X}_{(m)}$ is treated as a Gaussian generative model with I_m variables and $I_1 I_2 \ldots I_M$ observations and parameters $\boldsymbol{\mu}_m$ and $\boldsymbol{\Sigma}_m$ [12]. The corresponding probabilistic distance measure is defined as

$$d_{\mathrm{KL}} = \mathrm{KL}\Big(p(\boldsymbol{X}_m|\boldsymbol{\mu}_m, \boldsymbol{\Sigma}_m) \| q(\boldsymbol{X}'_m|\boldsymbol{\mu}'_m, \boldsymbol{\Sigma}'_m)\Big), \tag{5}$$

where the Kullback-Leibler divergence between two Gaussian distributions $\mathcal{N}_0(\boldsymbol{\mu}_0, \boldsymbol{\Sigma}_0)$ and $\mathcal{N}_1(\boldsymbol{\mu}_1, \boldsymbol{\Sigma}_1))$ is $\frac{1}{2}\big(\mathrm{tr}(\boldsymbol{\Sigma}_1^{-1}\boldsymbol{\Sigma}_0) + (\boldsymbol{\mu}_1 - \boldsymbol{\mu}_0)^\top \boldsymbol{\Sigma}_1^{-1}(\boldsymbol{\mu}_1 - \boldsymbol{\mu}_0) - k + \ln \frac{\det \boldsymbol{\Sigma}_1}{\det \boldsymbol{\Sigma}_0}\big)$ [14].

Kernels on the manifold of SPD matrices: Different metrics on the manifold of SPD matrices $\mathcal{S}_{++}^n$ may be used to define positive definite kernels [15]. The log-Euclidean metric $\| \ln \boldsymbol{\Sigma}_0 - \ln \boldsymbol{\Sigma}_1\|_{\mathrm{F}}$ corresponds to the geodesic distance between two SPD matrices $\boldsymbol{\Sigma}_0$ and $\boldsymbol{\Sigma}_1$, e.g. the shortest path between two elements on the manifold. It yields the corresponding distance

$$d_{\mathrm{logSPD}} = \| \ln(\mathrm{cov}(\boldsymbol{X}_m)) - \ln(\mathrm{cov}(\boldsymbol{X}'_m))\|_{\mathrm{F}}, \tag{6}$$

where $\mathrm{cov}(\boldsymbol{X}_m) \in \mathbb{R}^{I_m \times I_m}$ is the covariance matrix of $\boldsymbol{X}_m$. Similarly, we exploit the non-geodesic metric $\|\boldsymbol{\Sigma}_0 - \boldsymbol{\Sigma}_1\|_{\mathrm{F}}$ yielding the distance

$$d_{\mathrm{SPD}} = \|\mathrm{cov}(\boldsymbol{X}_m) - \mathrm{cov}(\boldsymbol{X}'_m)\|_{\mathrm{F}}. \tag{7}$$

Kernel on the Grassmann manifold: The Grassmann manifold $\mathcal{G}_{n,p}$ is the space of p-dimensional subspaces in a n-dimensional Euclidean space. In this manifold, it is not possible to find a geodesic distance that yields a positive definite kernel [15]. We use the non-geodesic projection or Chordal metric $\|\boldsymbol{Y}_0\boldsymbol{Y}_0^\top - \boldsymbol{Y}_1\boldsymbol{Y}_1^\top\|_{\mathrm{F}}$, where $\boldsymbol{Y}_0, \boldsymbol{Y}_1 \in \mathcal{G}_{n,p}$ to define the projection Gaussian kernel or Chordal distance-based kernel with

$$d_{\mathrm{Chordal}} = \|\boldsymbol{V}_m\boldsymbol{V}_m^\top - \boldsymbol{V}'_m\boldsymbol{V}'^\top_m\|_{\mathrm{F}}. \tag{8}$$

Here, $\boldsymbol{V}_m$ corresponds to the right orthonormal vectors of the SVD decomposition of the mode-m unfolding $\boldsymbol{X}_m$.

EXPERIMENT

In order to test the applicability and accuracy of the presented technique, we applied it to the dataset presented in [5]. We give here a very short description of the materials and methods used, see the original paper for details.

Experimental setup

The device used to capture muscles bulging around the full circumference of the arm is a shape-conformable tactile bracelet. The bracelet uses high-performance resistive elastomer-based tactile sensor technology, built upon the fact that the interface resistivity between two electrodes changes according to the applied load. The layout of the bracelet is such that a total number of 320 pressure sensors, arranged in a 8×40 torus shape around the forearm, gather a high-spatial-resolution (5mm) "pressure image" exerted by the deformation of the muscles engaged in moving the hand and wrist. The idea in itself is well-known, initially invented and studied by Craelius and others [16, 17], and its effectiveness is being studied with remarkable results, even when tested on amputated subjects [18]. TMG can be seen as a high-resolution version of force myography as laid out in the mentioned papers; Radmand et al. [19] provide a striking example of TMG applied to intact subjects, showing excellent classification accuracy. In order to provide a better form of simultaneous and proportional control, we hereby focus upon regression instead of classification.

In the experiment reported in [5], the ground truth was obtained by simply using the values of an animated visual stimulus, namely a hand model with nine degrees of freedom, with the understanding that the subjects would follow it with reasonable accuracy. This is an instance of *on-off goal-directed training*, already successfully employed, e.g., in [20, 21]. Such a method has the drawback of potentially reducing the precision in the prediction of the intended activations due to the delay required by the subject to adapt; nevertheless, it is an accepted way to associate an intended activation with a specific input signal pattern; in the case of amputees, it is actually the only possible way, since amputees cannot produce reliable ground truth in principle.

Participants and experimental protocol

The dataset was gathered from 10 intact subjects induced to follow movements of a realistic 3D hand model displayed on a monitor. The sequence of movements consisted of thumb rotation, flexion of the index and little finger, wrist flexion, extension and supination as shown by Fig. 1a. Each participant repeated this sequence of movements ten times while sitting in front of a monitor (see Fig. 1b).

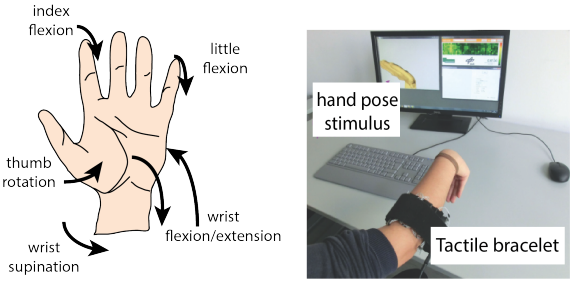

(a) (b)

Figure 1: (a) Movements executed by the participants. (b) A bird's eye view of the experimental setup used in [5] (reproduced with permission).

EXPERIMENTAL RESULTS

Table 2: Number of participants for which each method performed best per movement.

Metric	Thumb	Index	Little	Wr. flex	Wr. ext.	Wr. sup.
d_{Eucl}	1	4	4	**6**	3	**6**
d_{KL}	**8**	**6**	**5**	2	**4**	3
d_{SPD}	1	-	1	1	3	-
d_{logSPD}	-	-	-	1	-	1
d_{Chordal}	-	-	-	-	-	-

We applied tensor Gaussian Process Regression using RBF kernels based on Kullback-Leibler divergence (d_{KL}), Euclidean metric on $\mathcal{S}_{++}$ (d_{SPD}), log-Euclidean metric on $\mathcal{S}_{++}$ (d_{logSPD}) and Chordal distance (d_{Chordal}) in order to predict the visual stimulus values from the tactile bracelet. We compared the different results with those obtained by applying Ridge Regression (*RR*), equivalent to regularized least squares regression, and Gaussian process with the standard Euclidean metric computed by vectorizing the input data $d_{\text{Eucl}} = \|\text{vec}(\boldsymbol{X}_{(m)}), \text{vec}(\boldsymbol{X}'_{(m)})\|^2$. Cross-validation was applied to obtain a statistically significant estimation. The entire dataset for each participant and movement was randomly shuffled, then 10% of it was used to train each model and the test was performed on the remaining 90%. This procedure was repeated 50 times with a different random shuffle each time.

Table 1 shows three examples of typical average and standard deviation of the normalized root-mean-square error (NRMSE) values obtained by applying the different regression methods for each movement. The NRMSE values for Ridge Regression range from 1% to 11% depending on the movements and participants. This is in line with the values found by Koiva et al. [5]. As expected, all kernel methods achieve better results than Ridge Regression as they can encode nonlinear relationships. The NRMSE values of kernel methods range from 0.5% to 7.5% in function of the movements and participants.

We then compared the efficiency of the different kernel methods for each movement. Table 2 shows the number of participants for which each method performed best per movement. We observe that GP regression using the Euclidean metric and tensor GP regression with KL divergence-based kernel perform the best detection in most of the cases. Tensor GP regression with KL divergence-based kernel is generally the most efficient method to predict finger movement, especially thumb rotation, for most of participants. However, GP with Euclidean-based kernel seems more suitable to detect wrist movements.

DISCUSSION AND CONCLUSION

In this paper, we studied different kernels for tensor Gaussian Processes regression to detect hand and wrist activity by observing muscles bulging in the forearm. The paper concentrated on comparing several regression methods to data obtained in a previous experiment. The results presented above indicate that TMG data obtained from the forearm using the tactile bracelet can be effectively used to obtain *graded* muscle activations — as opposed to classification. As expected, due to the location of involved muscles, NRMSE values for movement involving the wrist are generally better predicted than the fingers movements, and errors in the prediction of thumb rotation are slightly higher. The slightly better results obtained by GP with Euclidean-based kernel on the wrist movements may be explained by the fact that muscles activation are more difficult to measure for finger movements, so that taking the structure of the data in account improves the detection of movements inducing patterns more difficult to distinguish.

All in all, it seems reasonable to claim that such a rich flow of information as the one obtained using 320 tactels (as opposed to the traditional sEMG schema in which a few sensors are involved) can provide better control than the state of the art; particularly, simultaneous and proportional control would greatly benefit from regression applied to TMG data. The results are promising, with all kernels methods being able to predict the different movements with an accuracy superior to previous approaches. Accounting for the structure and geometry of the data proved to be particularly helpful to detect finger movements.

ACKNOWLEDGEMENTS

This work was partially supported by the DFG/SNSF project "TACT-HAND: Improving control of prosthetic hands using tactile sensors and realistic machine learning" (Sachbeihilfe CA1389/1-1, Swiss National Science Foundation project 200021E-160665).

Table 1: Normalised root-mean-square error [%] for three participants and each performed movement. The lowest NRMSE for each movement and each participant is highlighted.

Participant 1	Thumb	Index	Little	Wr. flex	Wr. ext.	Wr. sup.
RR	6.75 ± 0.59	7.16 ± 0.55	7.79 ± 0.67	4.54 ± 0.40	4.03 ± 0.58	2.64 ± 0.31
GP, d_{Eucl}	3.79 ± 1.12	2.69 ± 0.43	2.70 ± 0.38	$\mathbf{2.75 \pm 0.67}$	1.86 ± 0.51	$\mathbf{1.19 \pm 0.20}$
TGP, d_{KL}	$\mathbf{2.80 \pm 1.25}$	$\mathbf{1.54 \pm 0.50}$	$\mathbf{1.86 \pm 0.47}$	3.73 ± 1.38	$\mathbf{1.56 \pm 0.50}$	$\mathbf{1.19 \pm 0.46}$
TGP, d_{SPD}	3.66 ± 0.70	2.86 ± 0.50	2.89 ± 0.51	2.94 ± 0.90	1.98 ± 0.52	1.43 ± 0.31
TGP, d_{logSPD}	3.88 ± 0.97	2.94 ± 0.47	2.99 ± 0.54	3.07 ± 0.66	2.09 ± 0.45	1.45 ± 0.29
TGP, d_{Chordal}	3.96 ± 0.87	3.12 ± 0.56	3.10 ± 0.43	2.99 ± 0.73	2.40 ± 0.53	1.51 ± 0.25
Participant 3	Thumb	Index	Little	Wr. flex	Wr. ext.	Wr. sup.
RR	10.82 ± 0.71	9.58 ± 0.81	8.74 ± 0.84	4.61 ± 0.55	3.70 ± 0.26	3.01 ± 0.43
GP, d_{Eucl}	5.12 ± 0.97	$\mathbf{4.66 \pm 0.91}$	$\mathbf{3.98 \pm 0.74}$	$\mathbf{2.80 \pm 0.61}$	1.78 ± 0.22	1.91 ± 0.41
TGP, d_{KL}	7.46 ± 2.13	6.89 ± 1.04	4.75 ± 0.93	3.92 ± 0.86	3.25 ± 0.75	2.71 ± 0.58
TGP, d_{SPD}	$\mathbf{5.07 \pm 0.86}$	5.04 ± 0.92	4.10 ± 0.83	2.83 ± 0.50	$\mathbf{1.68 \pm 0.30}$	1.83 ± 0.47
TGP, d_{logSPD}	5.66 ± 1.13	4.78 ± 0.55	4.27 ± 0.62	3.35 ± 0.56	2.48 ± 0.38	$\mathbf{1.81 \pm 0.33}$
TGP, d_{Chordal}	5.45 ± 0.97	4.75 ± 0.62	4.20 ± 0.68	3.35 ± 0.47	2.75 ± 0.54	1.95 ± 0.39
Participant 6	Thumb	Index	Little	Wr. flex	Wr. ext.	Wr. sup.
RR	4.34 ± 0.25	4.58 ± 0.29	3.15 ± 0.20	1.05 ± 0.06	1.30 ± 0.11	0.98 ± 0.06
GP, d_{Eucl}	1.90 ± 0.35	1.70 ± 0.35	1.23 ± 0.23	0.67 ± 0.24	0.53 ± 0.12	0.45 ± 0.10
TGP, d_{KL}	$\mathbf{1.27 \pm 0.34}$	$\mathbf{1.11 \pm 0.45}$	$\mathbf{0.69 \pm 0.16}$	$\mathbf{0.60 \pm 0.91}$	$\mathbf{0.43 \pm 0.22}$	$\mathbf{0.34 \pm 0.14}$
TGP, d_{SPD}	2.08 ± 0.42	2.06 ± 0.44	1.35 ± 0.21	0.66 ± 0.24	0.48 ± 0.11	0.47 ± 0.08
TGP, d_{logSPD}	2.31 ± 0.33	2.15 ± 0.44	1.75 ± 0.26	0.59 ± 0.16	0.68 ± 0.17	0.65 ± 0.07
TGP, d_{Chordal}	2.13 ± 0.32	2.12 ± 0.34	1.67 ± 0.21	0.61 ± 0.09	0.77 ± 0.16	0.62 ± 0.078

REFERENCES

[1] B. Peerdeman, D. Boere, H. Witteveen, H. in t Veld R., H. Hermens, S. Stramigioli, H. Rietman, P. Veltink, and S. Misra, "Myoelectric forearm prostheses: State of the art from a user-centered perspective," *Journal of Rehabilitation Research & Development (JRRD)*, vol. 48, no. 6, 2011.

[2] S. Amsuess, I. Vujaklija, P. Goebel, A. D. Roche, B. Graimann, O. C. Aszmann, and D. Farina, "Context-dependent upper limb prosthesis control for natural and robust use," *IEEE Transactions on Neural Systems and Rehabilitation Engineering*, vol. 24, pp. 744–753, July 2016.

[3] A. Ameri, E. Scheme, E. Kamavuako, K. Englehart, and P. Parker, "Real-time, simultaneous myoelectric control using force and position-based training paradigms," *Biomedical Engineering, IEEE Transactions on*, vol. 61, pp. 279–287, Feb 2014.

[4] N. Jiang, H. Rehbaum, I. Vujaklija, B. Graimann, and D. Farina, "Intuitive, online, simultaneous, and proportional myoelectric control over two degrees-of-freedom in upper limb amputees," *IEEE Transactions on Neural Systems and Rehabilitation Engineering*, vol. 22, pp. 501–510, May 2014.

[5] R. Kõiva, E. Riedenklau, C. Viegas, and C. Castellini, "Shape conformable high spatial resolution tactile bracelet for detecting hand and wrist activity," in *Proceedings of ICORR - International Conference on Rehabilitation Robotics*, pp. 157–162, 2015.

[6] K. P. Murphy, *Machine Learning A Probabilistic Perspective*. MIT Press, Cambridge (Massachusetts), London (England), 2012.

[7] Q. Zhao, C. Caiafa, D. Mandic, Z. Chao, Y. Nagasaka, N. Fujii, L. Zhang, and A. Cichocki, "High order partial least squares (HO-PLS): A generalised multilinear regression method," *IEEE Transactions on Pattern Analysis and Machine Intelligence*, vol. 35, no. 7, pp. 1660–1673, 2013.

[8] M. Rogers, L. Li, and S. Russell, "Multilinear dynamical systems for tensor time series," in *Advances in Neural Information Processing Systems (NIPS)*, (Lake Tahoe, USA), 2013.

[9] G. Dubbelman, *Intrinsic Statistical Techniques for Robust Pose Estimation*. PhD thesis, University of Amsterdam, Netherlands, 2011.

[10] M. Moakher and P. Batchelor, "Symmetric positive-definite matrices: From geometry to applications and visualization," *Visualization and Processing of Tensor Fields*, pp. 285–298, 2006.

[11] A. Edelman, T. A. Arias, and S. Smith, "The geometry of algorithms with orthogonality constraints," *SIAM Journal of Matrix Anal. & Appl.*, vol. 20, no. 2, pp. 303–351, 1998.

[12] Q. Zhao, G. Zhou, T. Adali, L. Zhang, and A. Cichocki, "Kernelization of tensor-based models for multiway data analysis: Processing of multidimensional structured data," *IEEE Signal Processing Magazine*, vol. 30, no. 4, pp. 137–148, 2013.

[13] Q. Zhao, G. Zhou, L. Zhang, and A. Cichocki, "Tensor-variate Gaussian processes regression and its application to video surveillance," in *Proc. IEEE Intl Conf. on Acoustics, Speech and Signal Processing (ICASSP)*, (Florence, Italy), 2014.

[14] J. Duchi, "Derivations for linear algebra and optimization," tech. rep., University of California, Berkeley, 2007.

[15] S. Jayasumana, R. Hartley, M. Salzmann, H. Li, and M. Harandi, "Kernel methods on Riemannian manifolds with Gaussian RBF kernels," *IEEE Trans. on Pattern Analysis and Machine Intelligence*, vol. 37, no. 12, pp. 2464–2477, 2015.

[16] M. Wininger, N. Kim, and W. Craelius, "Pressure signature of forearm as predictor of grip force," *Journal of Rehabilitation Research and Development (JRRD)*, vol. 45, no. 6, pp. 883–892, 2008.

[17] D. A. Yungher, M. T. Wininger, J. Barr, W. Craelius, and A. J. Threlkeld, "Surface muscle pressure as a measure of active and passive behavior of muscles during gait," *Medical Engineering & Physics*, vol. 33, no. 4, pp. 464–471, 2011.

[18] E. Cho, R. Chen, L.-K. Merhi, Z. Xiao, B. Pousett, and C. Menon, "Force myography to control robotic upper extremity prostheses: A feasibility study," *Frontiers in Bioengineering and Biotechnology*, vol. 4, p. 18, 2016.

[19] A. Radmand, E. Scheme, and K. Englehart, "High-density force myography: A possible alternative for upper-limb prosthetic control," *J Rehabil Res Dev.*, vol. 53, no. 4, pp. 443–456, 2016.

[20] D. Sierra González and C. Castellini, "A realistic implementation of ultrasound imaging as a human-machine interface for upper-limb amputees," *Frontiers in Neurorobotics*, vol. 7, no. 17, 2013.

[21] I. Strazzulla, M. Nowak, M. Controzzi, C. Cipriani, and C. Castellini, "Online bimanual manipulation using surface electromyography and incremental learning," *IEEE Transactions on Neural Systems and Rehabilitation Engineering*, vol. 25, no. 3, pp. 227–234, 2017.